JOURNAL OF BIOMOLECULAR STRUCTURE AND DYNAMICS
https://doi.org/10.1080/07391102.2020.1781694

Remdesivir (GS-5734) as a therapeutic option of 2019-nCOV main protease – *in silico* approach

Vankudavath Raju Naik[a], Manne Munikumar[b], Ungarala Ramakrishna[c], Medithi Srujana[d], Giridhar Goudar[e], Pittla Naresh[b], Boiroju Naveen Kumar[f] and Rajkumar Hemalatha[g]

[a]Extension and Training Division, ICMR-National Institute of Nutrition, Hyderabad, India; [b]NIN-TATA Centre for Excellence in Public Health Nutrition, ICMR-National Institute of Nutrition, Hyderabad, India; [c]Food Safety Division, ICMR-National Institute of Nutrition, Hyderabad, India; [d]Symbiosis Institue of Health Sciences, Symbiosis International (Deemed University), Pune, India; [e]Food Quality Analysis and Biochemistry Division, Biochem Research and Testing Laboratory, Dharwad, India; [f]Biostatistics Division, ICMR-National Institute of Nutrition, Hyderabad, India; [g]Division of Clinical Epidemiology, ICMR-National Institute of Nutrition, Hyderabad, India

Communicated by Ramaswamy H. Sarma

ABSTRACT

2019 – Novel Coronavirus (2019-nCOV), enclosed large genome positive-sense RNA virus characterized by crown-like spikes that protrude from their surface, and have a distinctive replication strategy. The 2019-nCOV belongs to the Coronaviridae family, principally consists of virulent pathogens showing zoonotic property, has emerged as a pandemic outbreak with high mortality and high morbidity rate around the globe and no therapeutic vaccine or drugs against 2019-nCoV are discovered till now. In this study, *in silico* methods and algorithms were used for sequence, structure analysis and molecular docking on M^{pro} of 2019-nCOV. The co-crystal structure of 2019-nCOV protease, 6LU7 have ~99% identity with SARS-CoV protease. The 6LU7 residues, Cys145 and His164 are playing a significant role in replication and are essential for the survival of 2019-nCOV. Alongside, 2019-nCOV M^{pro} sequence is non-homologous to human host-pathogen. Complete genome sequence analysis, structural and molecular docking results revealed that Remdesivir is having a better binding affinity with -8.2 kcal/mol than the rest of protease inhibitors, and peptide. Remdesivir is strongly forming h-bonds with crucial M^{pro} residues, Cys145, and His164. Further, MD simulation analysis also confirmed, that these residues are forming H-bond with Remdesivir during 100 ns simulations run and found stable (~99%) by RMSD and RMSF. Thus, present *in silico* study at molecular approaches suggest that, Remdesivir is a potent therapeutic inhibitor against 2019-nCoV.

List of Abbreviations: (2019-nCOV): 2019 novel coronavirus; (CoV): Coronavirus; (HE): Hemagglutinin-Esterase; (M^{pro}): Main protease; (MERS): Middle East Respiratory Syndrome; (MD): Molecular Dynamics; (NPT): Number of atoms, Pressure, Temperature; (PDB): Protein Data Bank; (rGyr): Radius of Gyration; (RdRp): RNA-dependent RNA polymerase; (RMSD): Root Mean Square Deviation; (RMSF): Root Mean Square Fluctuation; (SARS): Severe Acute Respiratory Syndrome; (SARS-CoV-2): Severe Acute Respiratory Syndrome Coronavirus 2; (SEA): Simulation Event Analysis; (SQA): Simulation Quality Analysis; (SASA): Solvent-Accessible Surface Area

ARTICLE HISTORY
Received 17 May 2020
Accepted 3 June 2020

KEYWORDS
2019-nCOV; COVID-19; Remdesivir; sequence analysis; phylogeny; molecular docking; dynamics simulations

Introduction

At first, an unknown case of pneumonia was detected in Wuhan, China, and was communicated to the World Health Organization (WHO) country office, China, on 31 December 2019. After a thorough examination, it was identified as a Coronavirus (CoV), a zoonotic virus that causes a range of illnesses including Middle East Respiratory Syndrome (MERS) and Severe Acute Respiratory Syndrome (SARS). SARS, due to SARS-CoV was initially identified in 2002, while MERS emerged in 2012, which was caused by MERS-CoV infection. The most recent coronavirus, Severe Acute Respiratory Syndrome Coronavirus 2 (SARS-CoV-2), provisionally called 2019 novel coronavirus (2019-nCOV), was never known to be identified in humans previously. However, the outbreak did not confine to China, rapidly spread to other parts of the world and soon WHO has recognized 2019-nCOV as pandemic on 11 March 2020. Besides, it is also the seventh and newest member of the Coronavirus which reports to be infectious to humans (Zhu et al., 2020). Currently, 4,647,961 confirmed cases and 308,985 total deaths due to 2019-nCOV had been reported worldwide as on 04 May 2020 (WHO). In India, the latest statistics by the Ministry of Health and Family Welfare have reported 85,940 and 30,153 total confirmed cases and deaths respectively (www.mohfw.gov.in).

CONTACT Manne Munikumar mannemunikumar.bioinfo@gmail.com Scientist-C (Bioinformatics), NIN-TATA Centre for Excellence in Public Health Nutrition, ICMR-National Institute of Nutrition, Jamai-Osmania (Post), Hyderabad, Telangana 500007, India; Vankudavath Raju Naik naik.vivaswan@icmr.gov.in Extension and Training Division, ICMR-National Institute of Nutrition, Jamai-Osmania (Post), Hyderabad 500007, Telangana, India

Supplemental data for this article can be accessed online at https://doi.org/10.1080/07391102.2020.1781694.

The contagious virus 2019-nCOV can spread primarily through the viral droplets of saliva and discharges from the nose of the infected person while coughing or sneezing and also touching contaminated surfaces (Pant et al., 2020). The typical viral infection symptoms of 2019-nCoV are dry cough, running nose, fever, shortness of breath in majority of cases. Some cases reported severe conditions such as pneumonia, severe acute respiratory distress syndrome, kidney failure with fatal consequences (Elfiky, 2020). However, as of now, there is no vaccine against this virus, which is the cause of the utmost trepidation globally. Nevertheless, the scientific fraternity all over the world has commenced with assiduous research work to understand the nature of virus, which may subsequently lead to the discovery of medicine and vaccine. However, several researchers have recognized that to investigate the routes of viral spread among humans, the site of activation must be identified. This led to identify the sites of various viruses including influenza family virus which enable uninterrupted spread of virus (Hasan et al., 2020).

The first line of treatment is targeted to treat the symptoms of the disease. Most of the symptoms of individuals affected with 2019-nCOV were similar to influenza, and both viruses cause respiratory issues. Influenza is a communicable disease caused by the influenza virus. This RNA virus contains seven genera: *Influenzavirus A, Influenzavirus B, Influenzavirus C, Influenzavirus D, Isavirus, Thogotovirus,* and *Quaranjavirus.* Among these, *Influenzavirus A, Influenzavirus B, Influenzavirus C* can infect humans. The *Influenzavirus A* virus is the most virulent human pathogens and can cause flu pandemics (Kumar et al., 2018). In humans, some of the serotypes which are known to cause pandemic deaths are H1N1 (known to cause Spanish flu and Swine flu), H1N2 (endemic in humans and pigs), H2N2 (Asian flu), H3N2 (Hong Kong flu), H5N1 (bird flu), H7N7 (unusual zoonotic potential), and H7N2 (low pathogenicity avian influenza virus) (Hay et al., 2001).

The study on viral composition revealed that the Hemagglutinin-Esterase (HE) glycoprotein gene is found in the beta coronaviruses, and this HE gene of coronaviruses have sequence homology with influenza HE glycoprotein and may reflect early recombination between the two viruses (Luytjes et al., 1988). Additionally, coronavirus spike (S) protiens can get attached to the human cell (especially lungs) surfaces via angiotensin converting enzyme (ACE2) receptors. Primarily, S1/S2 site in the coronavirus S protein is subjected to proteolytic cleavage by host proteases (trypsin and furin). Later, cleavage of S2′ site occurs which releases fusion peptide and triggers the activation of membrane fusion mechanism (Boopathi et al., 2020). Hence, it can be assumed that the mode of action of the drugs used in the treatment of influenza can work successfully in the same line to treat 2019-nCOV. Therefore, the clinical trials conducted revealed that most of the drugs inhibit the critical components of the 2019-nCoV life cycle. The lifecycle includes viral entry into the host cell, viral replication, and viral RNA synthesis (Boopathi et al., 2020). The previous research exertions to develop the anti-viral drugs against the Coronaviridae family receptors via, ACE2, RNA-dependent RNA polymerase (RdRp) and the main protease (M^{pro}, also called 3CLpro) proteins as potential drug targets. Among, M^{pro} as an attractive drug target among coronaviruses family which is essential and have a Signiant role in processing the polyproteins that are translated from the viral RNA (Anand et al., 2003; Hilgenfeld, 2014; Ton et al., 2020; Zhang et al., 2020). However, the M^{pro} protein sequence of 2019-nCoV is similar to the sequences of SARS-CoV and MERS-CoV proteins, which are mainly involved in the replication cycle (Harrison, 2020). Therefore, obstruction in the replication cycle may prove a suitable solution for the drug quest.

Since no specific therapy for 2019-nCOV is at-hand and considering public health priority, an immediate and effectual vaccine/drug is a crucial requisite. Gilead Sciences, Inc., United States (US), has started the first clinical trial to investigate the efficacy of Remdesivir, an adenosine analog which can cause pre-mature RNA termination of the nascent viral RNA. A double-blinded, placebo-controlled study (Remdesivir 200 mg intravenously administered for ten days, followed by 100 mg daily during hospitalization) was initiated along with, two phase-3 open-label randomized controlled trials simultaneously (https://www.pulmonologyadvisor.com/home/topics/$9#lung-infection/clinical-trials-underway-to-test-remdesivir-for-covid-19/; https://www.gilead.com/purpose/advancing-global-health/covid-19). However, Remdesivir has been accounted for to treat the first case of 2019-nCOV in the US effectively (Holshue et al., 2020).

Various provinces of China and India have initiated trials using Chloroquine or hydroxychloroquine, known anti-malarial agent, as a heme polymerase inhibitor (Rathi et al., 2020). It functions as a virus blocking agent via augmenting the endosomal, which is required for cell fusion and also by interfering with the glycosylation process of the cellular receptors of SARS-CoV (Vincent et al., 2005). Multiple types of studies (double blind, Phase 3, randomized, open-label and Phase 4, open-label, non-randomized) are at the initiation stage of recruiting study subjects. (http://www.chictr.org.cn/showproj.aspx?proj=48880).

Favipiravir an antiviral drug, known to effectively inhibit the 2019-nCOV infection in Vero E6 cells. An open-label non-randomized control study was conducted in the National Clinical Research Centre for Infectious Diseases Shenzhen, China, to assess the effectiveness of Favipiravir in 2019-nCOV treatment. The treatment showed significant assistance in terms of health progress by faster viral clearance and with further research, this can be considered as a standard treatment to combat the SARS-CoV-2 infection (Cai et al., 2020). Further, a randomized controlled trial of combined treatment of Favipiravir and Baloxavir Marboxil also carried out in Zhejiang, China (http://www.chictr.org.cn/showprojen.aspx?$9#proj=49013).

Wang et al. (2020) have evaluated seven antiviral drugs against a clinical isolate of 2019-nCoV *in vitro*. Among the seven tested drugs, high concentrations of three drugs, i.e. Ribavirin, Penciclovir, and Favipiravir, shown to lower the viral infection. Nafamostat, a potent inhibitor of MERS-CoV, was inhibitive against the 2019-nCoV infection since it prevents membrane fusion. Nitazoxanide, an anti-protozoal agent having potential antiviral property against a wide

range of coronaviruses also inhibited the 2019-nCoV at a low-micromolar concentration. Further, Remdesivir and Chloroquine were also found to be potently blocking virus infection at low-micromolar concentration.

Other antiviral drugs viz., Oseltamivir, and Zanamivir, which are neuraminidase inhibitors, are also under clinical trials. Efficacy of Oseltamivir (individually and in combination with other drugs) has been under interventional (Phase 3, clinical) trial to treat the 2019-nCoV Pneumonia in China and Thailand (https://clinicaltrials.gov/ct2/show/NCT04261270; https://clinicaltrials.gov/ct2/show/NCT04303299). Clinical trials for the various antiviral drugs are ongoing to find an effective treatment for 2019-nCoV. However, since the time-period estimated for the completion of the trials is too long, bioinformatics technology used to assess the efficacy of each drug individually at a molecular level and in complex with multiple probabilities. Hence, in view of the complex mechanisms associated with various drugs, there is a need to identify the drug which targets viral replication especially on the M^{pro} enzyme of 2019-nCoV. The most suitable drug/s predicted using bioinformatics tools and techniques may be used for further trials and may be prescribed for 2019-nCoV patients. Therefore, the current aim of the study is to dock the antiviral drugs (1) Remdesivir (2) Chloroquine (3) Favipiravir (4) Baloxavir Marboxil (5) Ribavirin (6) Penciclovir (7) Nafamostat (8) Nitazoxanide (9) Oseltamivir and (10) Zanamivir with M^{pro} to understand their effectiveness against 2019-nCoV. The findings of the present study with detailed molecular level empathetic of M^{pro} with potentiality-identified inhibitors might help in rational drug design to combat COVID-19.

Materials and method

Software and tools

Software and program used for the study involved PyMol (DeLano Scientific LLC, Palo Alto, California, USA) and Schrodinger Maestro 2020-1 (Academic license) (Maestro, Schrödinger, LLC, New York, NY, 2020) to visualize and modify receptor and inhibitor structures. MEGA X utilized for multiple sequences and phylogenic analyses. AutoDock 4.2 (The Scripps Research Institute, La Jolla, San Diego, USA) was used for the preliminary docking program in this study. The inhibitor PDBQT file format was prepared, and the grid box size was determined using AutoDock Tools version 1.5.4 (ADT; Scripps Research Institute, La Jolla, San Diego, USA).

Sequence analysis

According to the Centers for Disease Control and Prevention: CDC (https://www.cdc.gov/coronavirus/types.html) and World Health Organization: WHO (https://www.who.int/health-topics/coronavirus) the coronaviruses round outer surface has crown-like spikes. In humans, coronaviruses were first identified in the mid of 1960s (Killerby et al., 2018) around the globe and primary sub-groupings of coronaviruses are known as alpha, beta, gamma, and delta. Commonly infective human coronaviruses are 229E (alpha), NL63 (alpha), OC43 (beta), and HKU1 (beta). In last two decades SARS-CoV (2002) and MERS-CoV (2013) have evolved and now in 2019–2020, the novel coronavirus (2019-nCoV) has emerged as a pandemic outbreak (Chen, 2020; Lu et al., 2020; Yang et al., 2020; Yu et al., 2020). Recently, scientific reports have suggested that 2019-nCoV was evaluated from SARS-CoV and to be viewed as a new human-infective beta-coronavirus (Huang et al., 2020; Killerby et al., 2018; Yang et al., 2020).

Genome sequence comparison is essential to analyses the evolutionary relationship of viral genomes. With the swift growth of sequence and structure databanks, *in silico* approaches usually enforced to ascertain the functions and structures of unannotated sequences, and to explore the relationships between sequences. In this study, we retrieved seven M^{pro} FASTA sequence of coronaviruses (1) 229E: AGW80947 (2) NL63: AGT51371 (3) OC43: ATP16753 (4) HKU1: P0C6U4 (5) MERS-CoV: AUM60013 (6) SARS-CoV: AAY88865 and (7) 2019-nCoV: YP_009725295 from NCBI Viral genome database to discover the evolutionary relationship by phylogenetic tree construction was using MEGA X tool (Felsenstein, 1985; Kumar, Stecher, et al., 2018). For *in silico* analysis the first reported M^{pro} sequence from china, 2019-nCoV of YP_009725295 selected as a reference sequence.

Structure analysis

For the sequence YP_009725295, BLASTp analysis was performed to find the 3 D structure of the reference 2019-nCoV M^{pro} against the protein data bank (PDB). The co-crystal structure of 2019-nCoV (PDB ID: 6LU7) with an N3 peptide inhibitor (n-[(5-methylisoxazol-3-yl) carbonyl] alanyl-l-valyl-*n*∼1∼-((1r,2z) −4- (benzyloxy) −4- oxo-1-{[(3r)- 2-oxopyrrolidin-3-yl] methyl} but-2-enyl) -l-leucinamide) (Jin et al., 2020) with ∼306 amino acids have 100% identity with 2019-nCoV M^{pro} and was chosen as a reference structure for further molecular docking analysis. For validation, the obtained sequence and structure results of a similar sequence were equated with ClustalX (Higgins & Sharp, 1988) by performing pairwise sequence alignment with a 6LU7 amino acid sequence. The active-site residues of the 6LU7 M^{pro} complex with N3 were visualized by using PyMOL.

Lead identification

So far, there is no particular antibody and medications against 2019-nCoV. Specialists are presently taking a shot at various antiviral drugs, immunotherapies, and immunizations that are being researched to discover the potential treatment for 2019-nCoV. As of now, countless FDA approved antiviral agents are in use for the treatment of 2019-nCoV viral infection. However, numerous examples exist in which the utilization of a second antiviral agent would be advantageous because it would permit the choice of either option or a combination therapeutic approach. As 2019-nCoV infections have risen, the focus on encoded proteases to discover potent antiviral medications are in progress. Recent molecular studies have demonstrated that viral protease's existence

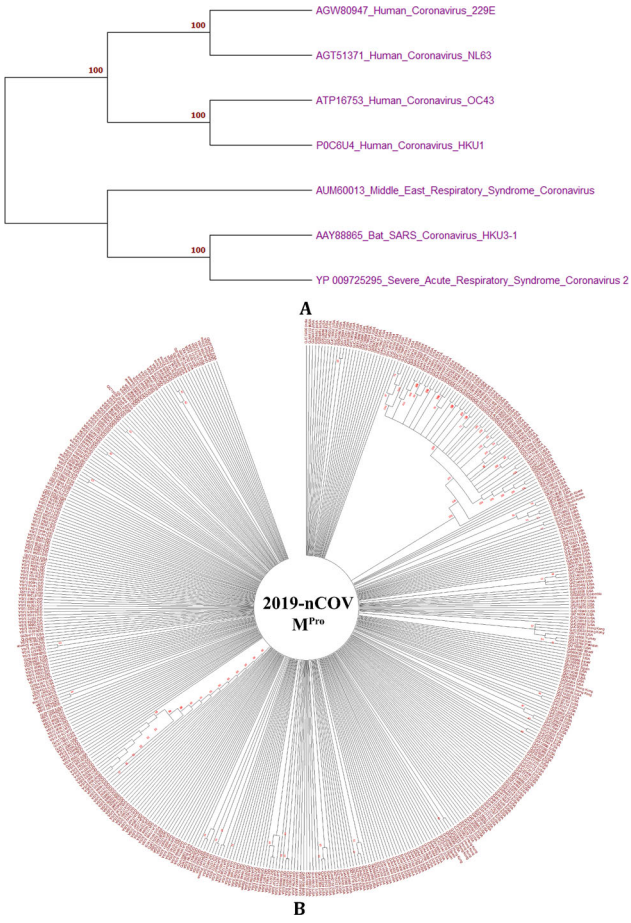

Figure 1. Phylogenetic tree of Coronavirus M^{pro}. (A) Three M^{pro} sequence of MARS-CoV (AUM60013), SARS-CoV (AAY88865) and 2019-nCoV (YP009725295) with four Human (AGW80947, AGT51371, ATP16753 and P0C6U4) Coronavirus. (B) Phylogenetic tree of 2019-nCoV M^{pro} (500 sequences).

pattern depends upon numerous infections by affecting the cleavage/catalyzing process of viral polyprotein antecedents (which are high molecular weight)/essential proteins important for assembly and morphogenesis of virus particles. Most of the chosen protease inhibitors are utilized principally for the treatment of Herpesvirus, Human Immunodeficiency Virus (HIV), Respiratory Syncytial Infection and flu A viruses, and can also be used for the treatment of 2019-nCoV.

In this scenario, sequence and structure analysis was performed for 2019-nCoV M^{pro} through BLAST, results revealed that M^{pro} nucleotide sequence has ~99% identity and ~40% of query coverage with SARS-CoV. As mentioned in the introduction section, Remdesivir, Chloroquine, Favipiravir, Baloxavir Marboxil, Ribavirin, Penciclovir, Nafamostat, Nitazoxanide, Oseltamivir and Zanamivir ae chosen for the molecular docking analysis and the same inhibitors retrieved from the PubChem database.

Molecular docking

Molecular docking perceived *in silico* structure-based strategy is broadly utilized in drug design and discovery approaches. Molecular docking empowers to identify novel compounds of therapeutic interest for the emerging pandemic infectious outbreaks by predicting the inhibitor-receptor interactions. Even though it initially evolved for assisting to understand the mechanism of molecular binding recognition among small compounds and receptor molecules, in recent years, uses and applications of molecular docking have profoundly changed to help in the rapid development of drug discovery (Khandare et al., 2018; Munikumar et al., 2019; Pradhan et al., 2014).

Protein structure preprocessing and optimization

Three-dimensional structure of 2019-nCoV M^{pro} with N3 peptide (PDB ID: 6LU7) was obtained from the protein data bank (PDB) (Jin et al., 2020) for molecular docking analysis. A fully automated docking software tool, AutoDock 4.2, which is most widely used to study the receptor-ligand binding and interactions, was used for the docking of selected inhibitors with 2019-nCoV M^{pro} structure. The receptor and ligand files were denoted in PDBQT file format, a modified PDB format containing atomic charges, atom type definitions for ligands, and topological information (rotatable bonds). Receptor molecule was initially fixed by adding polar hydrogen, Kollman charges (Azam & Abbasi, 2013; Morris et al., 2009). Selected inhibitor molecules were added with Gasteiger charges (Sliwoski et al., 2014). Autodock 4.2 allows setting a specific target site with the help of a grid box. The X, Y, and Z dimensions were set to 40*40*40, the X center, Y center, and Z center with a grid spacing of 1 Å, keeping the receptor rigid and the ligand as a flexible molecule was adjusted by N3 peptide-binding site of the 6LU7 (Jin et al., 2020). The output for each inhibitor's conformations was analyzed using a stochastic Lamarckian genetic algorithm (Morris et al., 2009). After characterizing the coupling site and receptor-ligand readiness, docking runs were propelled from the command prompt. The molecular interactions, the energy between every ligand and the receptor, was determined for the binding site, which expressed as affinity (kcal/mol) and favourable conformations. The 3 D visualization of docked structures was performed using a graphical user interface, Maestro Schrodinger 2020-1 (Khandare et al., 2018; Munikumar et al., 2019; Umamaheswari et al., 2011). Further, molecular dynamics simulations were performed with outmost docked complex and co-crystal structure (native) for the stability was close to biologically relevant characteristics.

Molecular dynamics simulations

Molecular dynamics (MD) simulations were carried out using the Desmond 2018-4 simulations module of Schrödinger LLC. To simulate the outmost docked complex and native co-crystal with N3 peptide, a simple point charge (SPC) of the HOH molecule model was accounted. Alongside, orthorhombic periodic boundary box (X, Y, and Z-axis) conditions were set up to specify the shape and size of the complex unit buffered at 10 Å distances. The docked complex was neutralized with the system electrically, by adding appropriate counter NA^{+}/Cl^{-} ions to balance the system charge and were placed randomly in the solvated system. After building the solvated system, protein-ligand complex minimization and relaxation

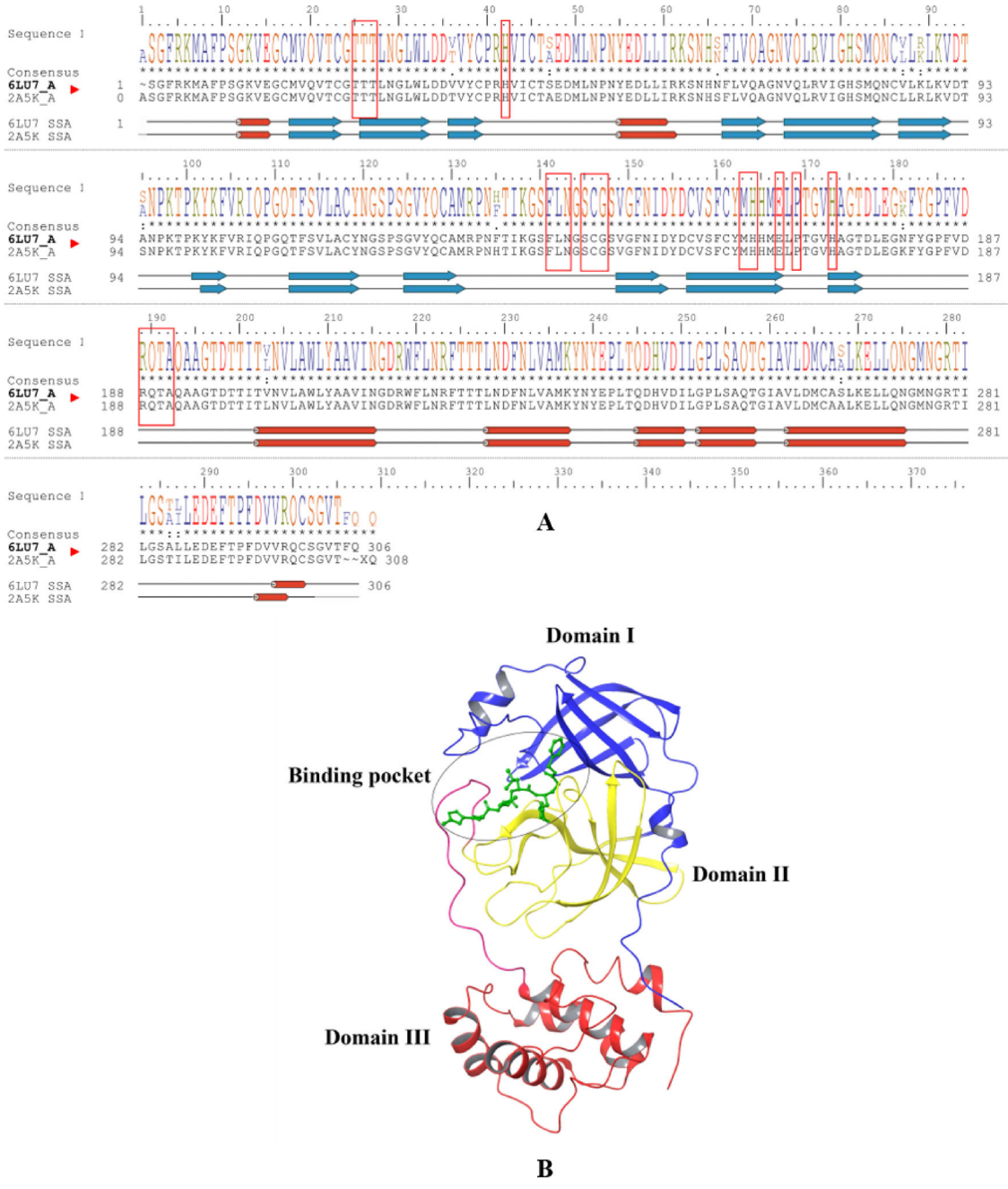

Figure 2. Sequence alignment of 2019-nCoV M^{pro} with SARS-CoV M^{pro}. (A) The secondary structure of peptidase in the alignment were assigned using Schrodinger maestro 2020-1. The N3 peptide binding residues for M^{pro} of 2019-nCoV are highlighted as red coloured box. (B) 2019-nCoV M^{pro} domains (domain-I: blue, domain-II: yellow, domain-III: red and loop: pink, between domain I and II and binding), with N3 peptide: green.

were performed under the constant Number of atoms, Pressure, Temperature (NPT) ensemble using Desmond's minimization & relaxation protocol that consists of nine stages (Vilar et al., 2011). The Stage 1: Perceive the initial simulation setup parameters, Stage 2: Minimization with restraints on the solute, Stage 3: Minimization without any restraints, Stage 4: Simulate with Berendsen NVT, $T = 10$ K, small-time step, and restraints on solute heavy atoms, Stage 5: Simulate with Berendsen NPT, the parameter was fixed $T = 10$ K, and restraints on solute heavy atoms, Stage 6: solvate pocket, Stage 7: simulate with Berendsen NPT and restraints on solute heavy atoms, Stage 8: Simulate with Berendsen NPT and no restraints, and Stage 9: Production time minimization at 100 ns with the periodic boundary conditions in the NPT ensemble using OPLS 2005 force field parameters and each production of trajectories was configured and observed at 4.8 ps intervals (Leimkuhler & Sweet, 2004).

The behaviour of each MD simulations trajectory files were analysed by using Simulation Quality Analysis (SQA), Simulation Event Analysis (SEA) tools of Desmond modules for calculating the potential energies, root-mean-square deviation (RMSD), root mean square fluctuation (RMSF), radius of gyration (rGyr), Solvent-Accessible Surface Area (SASA), and total intramolecular H-bonds contributing to the structural stability. The SQA and SEA are useful parameters to

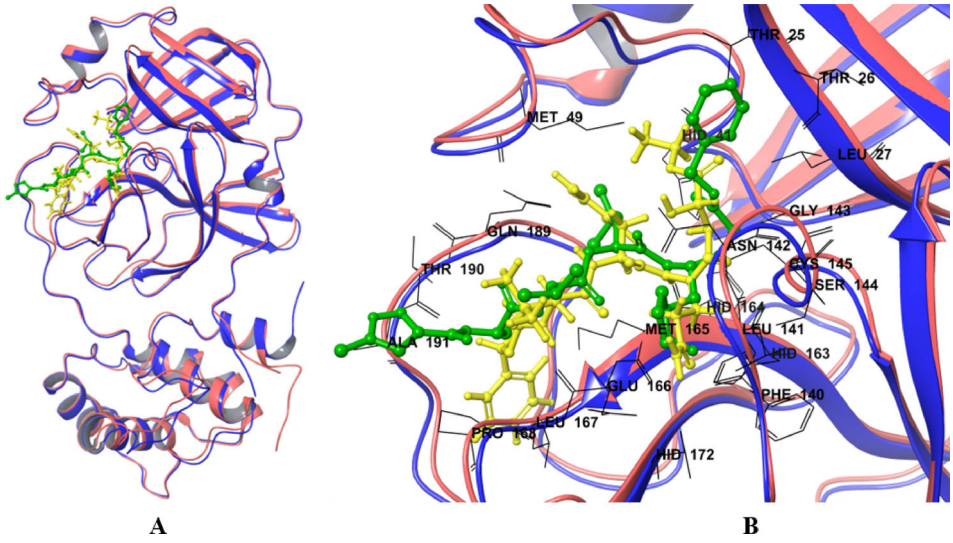

Figure 3. Molecular interactions of native and docked complexes. (A) Superimposition of native and docked 2019-nCoV; native 6LU7: cyan with N3 green and docked 6LU7: pink with N3: violet. (B) Molecular binding-site interactions (black) native and docked 2019-nCoV; native 6LU7: cyan with N3: violet, docked 6LU7: pink with N3: green within 4Å region.

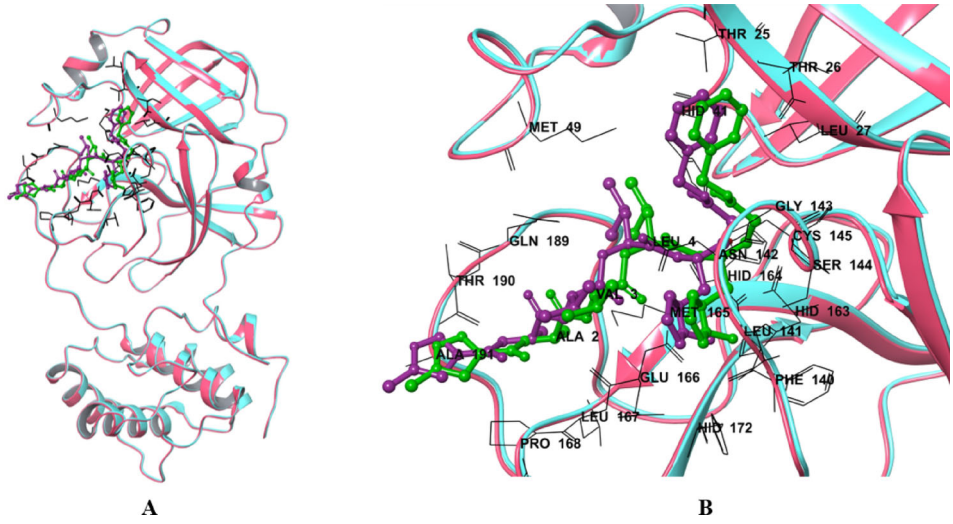

Figure 4. Structure superimposition of M^{pro} with peptides (N3 and AZA). (A) Superimposition of 2019-nCoV (6LU7: pink with N3 peptide: yellow) and SARS (2A5K: blue with AZA peptide: green). (B) Molecular binding-site interactions (black) within 4Å region; 2A5K (blue) with AZA peptide (green), 6LU7 (pink) with N3 peptide (yellow).

qualitatively validate the complex system stability throughout the 100 ns run and protein changes at the simulated length of chemical time for the given temperature, pressure, and volume of the total simulation box.

Results and discussion

Phylogenetic analysis

Multiple sequence alignment of the retrieved M^{pro} sequences was performed, and the phylogenetic tree was constructed using Mega-X (Felsenstein, 1985). The evolutionary history was inferred by applying the Maximum Likelihood method and the JTT matrix-based model. It is found that the tree is having the highest log-likelihood of 3.186 (Figure. 1) with selected seven M^{pro} sequences. The construction of initial tree(s) for the heuristic search were obtained automatically by enforcing with Neighbor-Join and BioNJ algorithms, and JTT model used for estimating matrix of pairwise distances to select the topology with superior log likelihood value. The constructed phylogeny tree is drawn to scale, with branch lengths measured in the number of substitutions per site of sequence. The proportion of each sites in which at least one unambiguous base was present, in at least one sequence for each descendent clade, was shown next to each internal node in the tree. For interim datasets preparation, a total of 7444 pair-wise positions were constituted with seven M^{pro} sequences for phylogeny analysis. The resultant trees were evaluated by 500 bootstrap replicates (Felsenstein, 1985).

The alignment shows that amongst the seven M^{pro} protein sequences identical with BAT SARS-CoV, four sequences are from different Human Coronaviruses isolates, one from MERS CoV and one from BAT SARS CoV isolate. Notably, the 2019-nCoV of M^{pro} is identical (100%) with BAT SARS-CoV

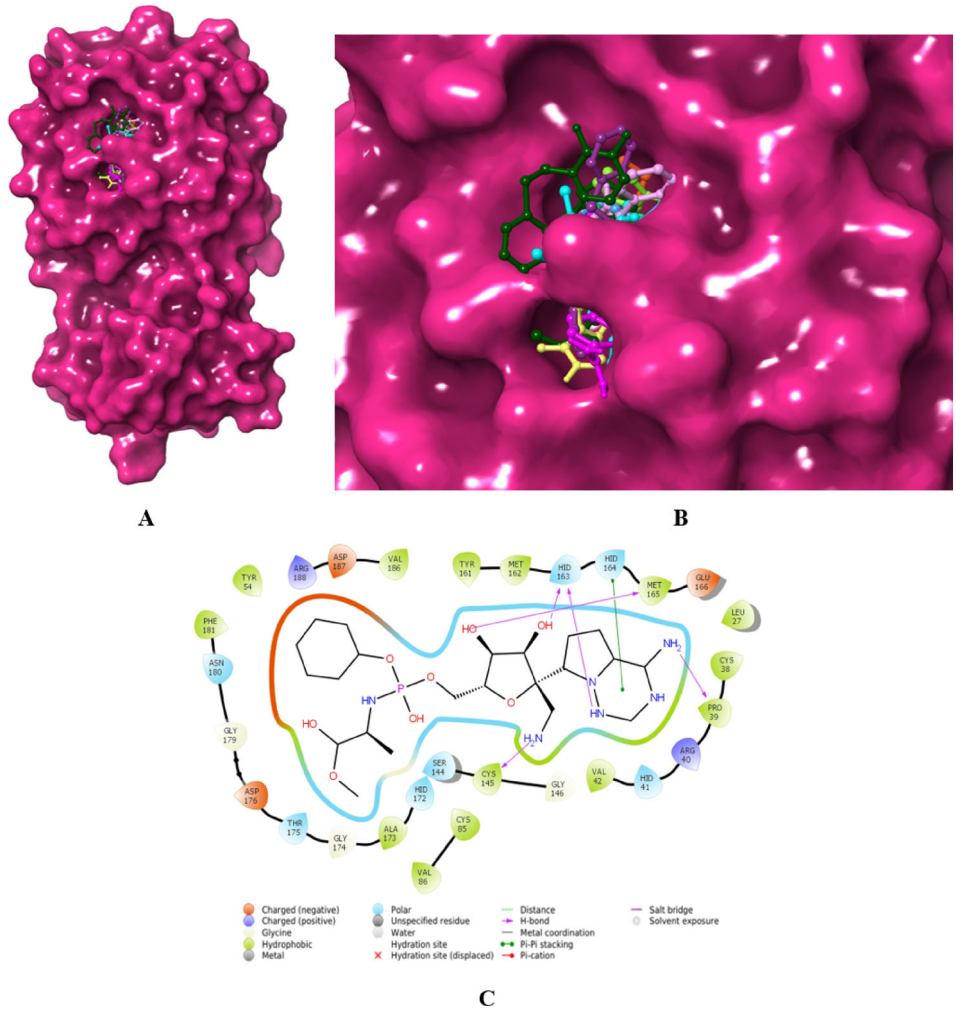

Figure 5. Docking complex and molecular interactions of Mpro and selected inhibitors (A) The overall M^{pro}3D docked complex with selected inhibitors (B) Binding site of M^{pro} with inhibitors (C) Molecular binding site interactions of Remdesivir docked to 2019-nCoV M^{pro} complex within 4Å region.

and distantly related (∼34%) to Human Coronavirus, 229E (Figure 1A). Results suggest that M^{pro} of 2019-nCoV was evolved from BAT SARS-CoV.

Further, phylogenetic analysis is performed with 500 M^{pro} protein sequence from the NCBI viral genome database (till 4th May 2020) (Figure 1B). The results show that a minimum of 51% evolutionary relationship was observed among the geographically distributed M^{pro} protein sequences.

Structure determination

The 2019-nCoV is an enveloped positive-sense single-strand RNA virus, infecting primarily respiratory system. It also infects the gastrointestinal epithelial cells, macrophages, and other cell types, thereby triggering the systemic changes and damage to many vital organs for instance lung, heart, liver, kidney and adrenal gland. Anti-2019-nCoV therapeutics could target several major viral pathogeneses, such as virus-cell interactions, virus entry, intracellular viral replication, and virus assembly and exit (Lu, 2020; Medhi et al., 2020). The intracellular replication of 2019-nCoV was mediated by "replicase" complex derived from virally coded polyprotein precursor of M^{pro} (306 AA). 2019-nCoV and SARS-CoV-2 M^{pro} proteins share ∼99% identity in amino acid sequences and ∼100% binding site (Figure 2A).

Importantly, M^{pro} protein of SARS-CoV-2 and SARS-CoV have a high degree of homology in three domains (Figure 2B) (1) domain I (residues 8 to 101), (2) domain II (residues 102 to 184) comprises of two-β-barrel fold similar to that of the chymotrypsin-type serine peptidases and, (3) domain III (residues 201 to 300) has five α-helices and is connected to domain II by a long loop (residues 185 to 200) (Jin et al., 2020).

Molecular docking

Validation of docking protocol (standardization)

To validate the docking protocol docking and superimposing the co-crystal structures of the 2019-nCoV M^{pro} and SARS CoV M^{pro} was done (Figures 3 and 4).

At first, the docking was performed with the co-crystal structure of 2019-nCoV i.e. M^{pro} with N3 peptide and the docked complex was superimposed with the native co-crystal structure, M^{pro} with N3 peptide complex, the superimposition has 0.923Å RMSD, which precisely coincided with each other (Figure 3A). Whereas, N3 peptide have ∼98% identical

Table 1. Molecular docking score, interactions and bond length of selected inhibitor with 2019-nCoV M^{pro}.

Ligand	Docking score (kcal/mol)	H-bond	H-bond Interactions (Å)	Interactions
Remdesivir	−8.2	Pro39:C = O → NH	1.10	Pro39, Thr25, Thr26, Leu27, Asn28, Gly29, Leu30,
		Cys145:C = O → NH	2.11	Tyr37, Cys38, Pro39, His41, Met49, Cys117, Tyr118,
		His163:C = O → OH	2.54	Asn119, Gly120, Phe140, Leu141, Asn142, Gly143,
		His163:NH → C = O	2.13	Ser144, Cys145, Gly146, Ser147, Met162, His163,
		His164:π-π	–	His164, Met165, Glu166
		Met165:NH → C = O	3.50	
Baloxavir marboxil	−7.8	His41: π-cation	–	Thr25, Thr26, Leu27, His41, Met49, Phe140, Leu141,
		Cys145:NH → CO	2.61	Asn142, Gly143, Ser144, Cys145, His163, His164,
		Glu166:NH → CO	2.26	Met165, Glu166, Gln189
Nafamostat	−7.7	Tyr54:CO ← NH	1.38	Leu27, Pro39, Arg40, His41, Yal42, Cys44, Met49,
		Phe140:C = O ← NH	1.48	Pro52, Tyr54, Tyr118, Phe140, Leu141, Asn142,
		Cys145:NH → CO	2.58	Gly143, Ser144, Cys145, His163, His164, Met165, Glu166, His172, Asp187, Arg188
Nitazoxanide	−6.7	Gly143:NH → CO	2.44	Val20, Thr25, Thr26, Leu27, Asm28, Pro39, Arg40,
		His164:NH ← NO	2.71	His41, Val42, Met49, Tyr54, Leu141, Asn142, Gly143, Ser144, Cys145, His164, Met165, Asp187
Penciclovir	−6.5	Tyr54:CO ← HN	2.64	Thr26, Leu27, His41, Met49, Tyr118, Phe140,
		Cys145:C = O → OH	2.48	Leu141, Asn142, Gly143, Ser144, Cys145, His163,
		Cys145:NH ← CO	1.54	His164, Met165, Glu166, His172, Gln189
Zanamivir	−6.5	His41:C = O ← NH	2.23	Thr25, Thr26, Leu27, Asn28, Pro39, Arg40, His41,
		Asn142:C = O ← OH	2.38	Yal42, Cys44, Met49, Cys117, Tyr118, Asn119,
		Cys145:C = O ← OH	2.58	Phe140, Leu141, Asn142, Gly143, Ser144, Cys145,
		His164:C = O ← NH	2.23	Gly146, Ser147, His163, His164, Met165, Glu166, Gln189
Ribavirin	−6.2	Ser144:NH → CO	2.80	His41, Met49, Leu141, Asn142, Gly143, Ser144,
		Cys145:NH → CO	2.31	Cys145, His163, His164, Met165, Glu166, Asp187,
		His164:C = O ← NH	2.43	Arg188, Gln189
Oseltamivir	−6.1	His41:NH → CO	2.68	Thr25, Thr26, Leu27, His41, Cys44, Met49, Tyr54,
		Cys145:NH → CO	2.74	Leu141, Asn142, Gly143, Ser144, Cys145, His163,
		Glu166:NH → CO	2.33	His164, Met165, Glu166, Asp187, Arg188, Gln189
Chloroquine	−5.7	Cys:145:CS ← NH	1.23	Leu27, Pro39, His41, Met49, Tyr54, Phe140, Leu141, Asn142, Gly143, Ser144, Cys145, His163, His164, Met165, Glu166, Val186, Asp187, Arg188, Gln189
Favipiravir	−5.0	Phe140:C = O → NH	2.07	Phe140, Leu141, Asn142, Gly143, Ser144, Cys145,
		His163:NH ← CO	2.19	His163, His164, Met165, Glu166, His172
N3 Peptide	−4.1	Phe140C = O → CN	3.19	Thr24, Thr25, Thr26, His41, Met49, Tyr54, Phe140,
		Gly143:CN → CO	2.87	Leu141, Asn142, Gly143, Ser144, Cys145, His163,
		Cys145:CS → C = O	2.32	His164, Met165, Glu166, Leu167, Pro168, His172,
		His163:CN → C = O	2.37	Asp187, Arg188, Gln189, Thr190, Ala191, Gln192
		His164:C = O → CN	2.80	
		Glu166:C = O← CN	2.83	
		Glu166:CN← C = O	2.98	
		Gln189:C = O → CN	2.98	
		Thr190:C = O→ CN	2.85	

interactions in a superimposed complex within a 4Å region of molecular binding-site of domains I and II (Figure 3B).

Second, as we have found that 2019-nCoV (PDB ID: 6LU7) M^{pro} have 100% sequence identity with BAT SARS-CoV (PDB ID: 2A5K), to validate the same using co-crystal structures, 2A5K with (5 s,8s,14r)-ethyl 11-(3-amino-3-oxopropyl)-8-benzyl-14-hydroxy-5-isobutyl-3,6,9,12-tetraoxo-1-phenyl-2-oxa-4,7,10,11-tetraazapentadecan-15-oate (AZA) peptide (Lee et al., 2005), with docked M^{pro} with N3 peptide complex was taken and superimposed (Figure 4A). The resulted docked complex was superimposed with the native co-crystal structure, 2A5K with AZA peptide, the superimposition has 1.029Å RMSD, which precisely coincided with each other (Figure 4B).

Third, superimposition has 0.095Å RMSD with ∼100% of conserved binding site residues of docked complex of 6LU7–N3 and co-crystal stricture of 2A5K–AZA was observed each other (Figure 3B). Further, validation of M^{pro} binding pocket, we obtained 84 co-crystal protein sequence of 2019-nCoV M^{pro} from the PDB (till 4 May 2020) (Supplementary Figure 1) and performed multiple sequence analysis (MSA) by exploring Schrodinger software. The results revealed that, binding site residues are 100% conserved amongst the geographically distributed M^{pro} protein sequences of 2019-nCoV.

The co-crystal M^{pro} with N3 peptide positioned in the cleft between domain I and II shares nine h-bonds with bond length (1) Phe140:3.19Å (2) Gly143:2.87Å (3) Cys145:2.32Å (4) His163:2.38Å (5) His164:2.80Å (6) Glu166:2.83Å (7) Glu166:2.98Å (8) Gln189:2.89Å and (9) Thr190:2.85Å, were observed in both native and docking complexes within 4Å radii. The Van Der Waals (VdW) interactions of Thr24, Thr25, Thr26, His41, Met49, Tyr54, Phe140, Leu141, Asn142, Gly143, Ser144, Cys145, His163, His164, Met165, Glu166, Leu167, Pro168, His172, Asp187, Arg188, Gln189, Thr190, Ala191, and Gln192 (Figure 5C) were also observed in both native and docking complexes within 4Å radii (Table 1).

The 100% conserved binding sites interactions and significant superimposed RMSD scores of the above docking approaches suggest that the AutoDock 4.2 software docking protocol could be used for the identification of potent

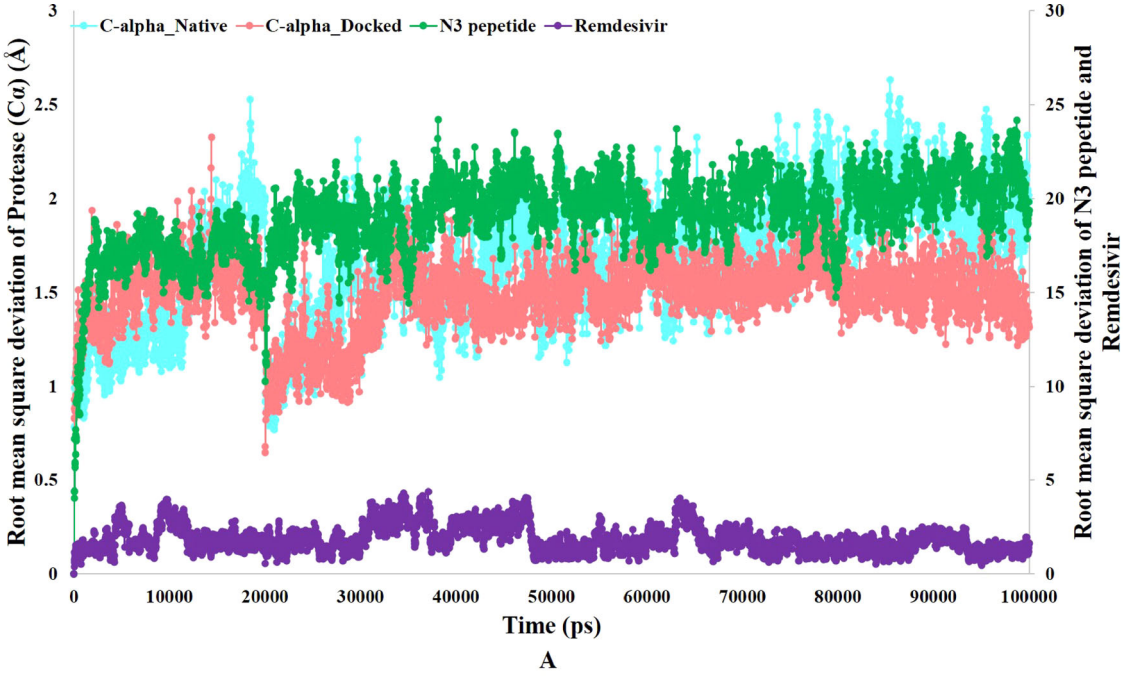

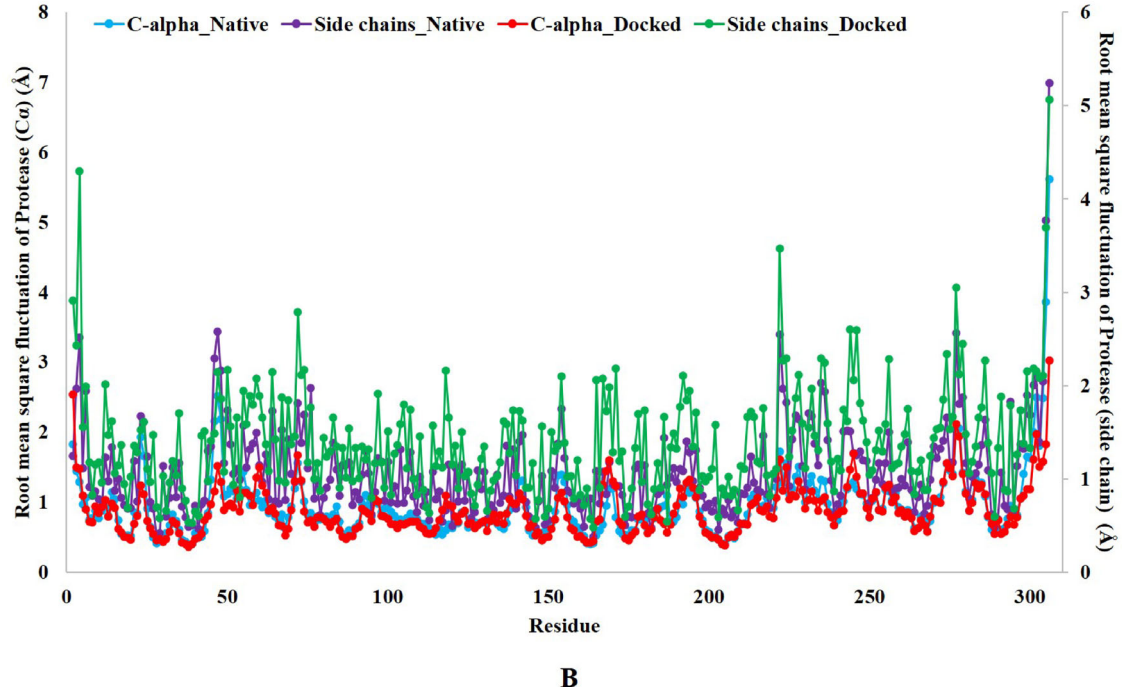

Figure 6. Molecular dynamics simulations analysis of docked (M^{pro} – Remdesivir) and native (M^{pro}– N3 peptide) complexes of 2019-nCoV M^{pro} during 100 ns period (A) RMSD plot of the docked and native (B) RMSF of docked and native (C) Radius of Gyration (rGyr) of docked and native complexes (D) Solvent Accessible Surface Area (SASA) of docked (M^{pro} – Remdesivir) (E) SASA of docked (M^{pro}– N3 peptide).

inhibitor (computer-aided drug designing/structure-based drug designing) for the novel drug discovery against 2019-nCoV.

Molecular interactions of M^{pro} with inhibitor

The docking complex of each M^{pro} inhibitors with 2019-nCoV M^{pro} was analysed by the Schrodinger maestro 2020-1 visualization tool. The selected anti-viral protease inhibitors led to the better docking score and binding interactions than N3 peptide within the cleft of domain I and domain II (Figure 2B). The results revealed that the protease inhibitors were having better molecular docking scores with a strong binding affinity with the M^{pro} of 2019-nCoV. The present study results also represented here are starting with better binding score to least binding score: Remdesivir > Baloxavir marboxil > Nafamostat > Nitazoxanide > Penciclovir > Zanamivir > Ribavirin > Oseltamivir > Chloroquine > Favipiravir (Table 1 and Figure 5A and B). Thus, the evidence from the molecular docking score and binding affinity suggested that these inhibitors are eminently interacting with 2019-nCoV M^{pro} and might be considered for therapeutic interventions of 2019-nCoV (Figure 5B).

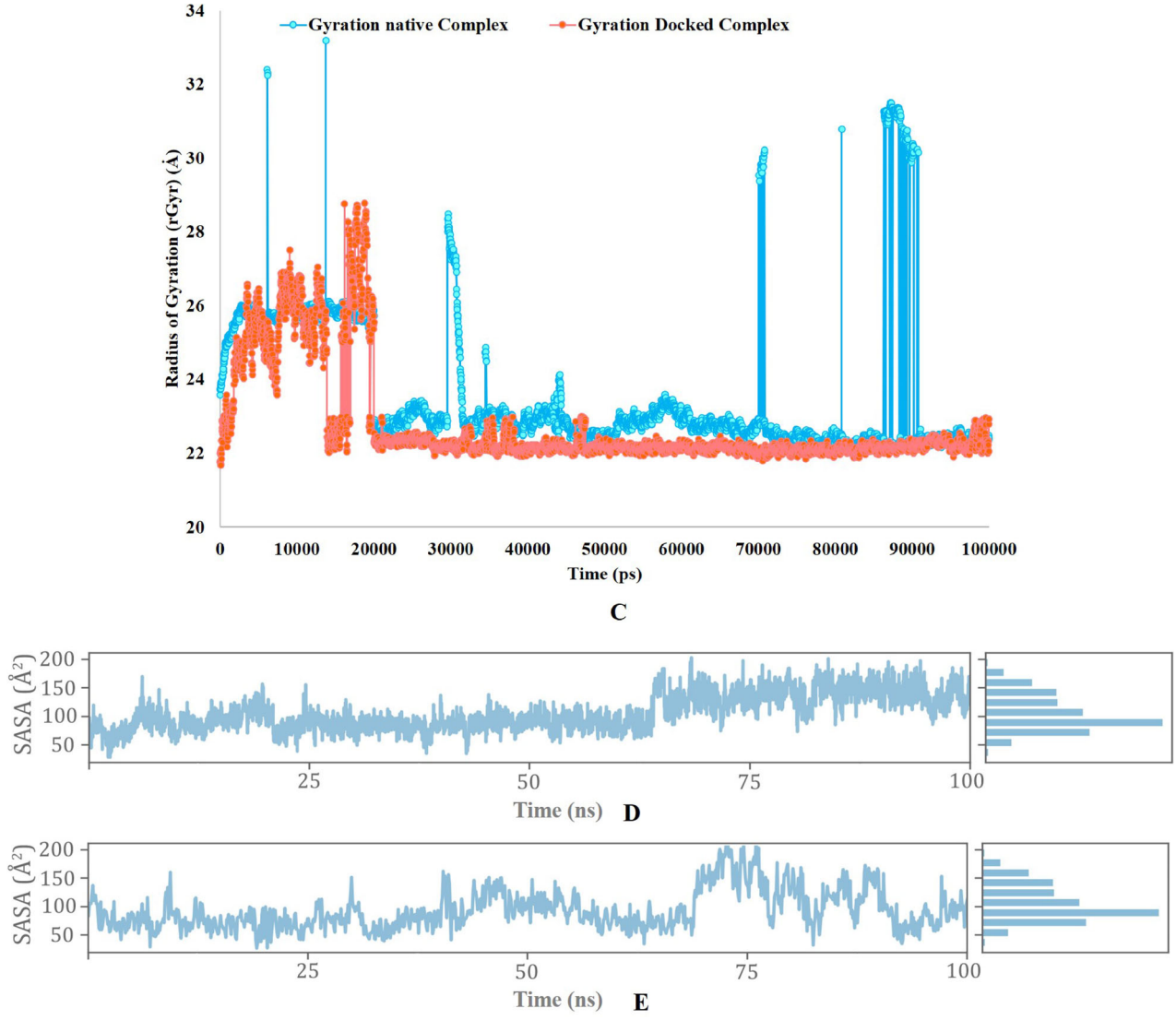

Figure 6. Continued

Among the inhibitors, the Remdesivir attributed to the best docking score (−8.2 kcal/mol) with greater number of h-bond (five) interactions and bond lengths with the following M^{pro} amino acid residues: (1) Pro39 (2) Cys145 (3) His163 (4) His163 and (5) Met165 (Figure 4A). Moreover, His164 formed π-π interaction with 1, 2, 4-triazinan-5-amine group of benzene ring (Figure 5C). The VdW interaction residues of Thr25, Thr26, Leu27, Asn28, Gly29, Leu30, Tyr37, Cys38, Pro39, His41, Met49, Cys117, Tyr118, Asn119, Gly120, Phe140, Leu141, Asn142, Gly143, Ser144, Cys145, Gly146, Ser147, Met162, His163, His164, Met165, and Glu166 were housed within 4Å of Remdesivir inhibitor.

Docked complex structure conformational stability and flexibility analysis through MD simulations

The conformational stability nature of docked (M^{pro} – Remdesivir) and native (M^{pro} – N3 peptide) complex system was entrenched with HoH, volume (V), temperature (T) and pressure (P) observed by MD simulation of 100 ns (Supplementary Figure 2). Each trajectory was analysed for stability conformation through RMSD, RMSF, rGyr, and H-bond monitoring (Figure 6). The docked and native complexes are depicted the average of total energy (−132446.36 and −99501.23 kcal/mol), potential energy (−162734.98 and −121628.90 kcal/mol) of the system was relatively stable with the average temperature (298.65 kelvin), pressure (1.88 bar), and volume (502884.87 and 362278.77 $Å^3$) throughout the simulations run (Supplementary Figure 2). The RMSD during the simulations period was analysed for M^{pro} Cα – Remdesivir complex had an average of 1.48 Å and 1.86 Å respectively. The average RMSD for native M^{pro} Cα – N3 peptide complex was 1.65 Å and 19.09 Å respectively (Figure 6A). By contrast, native N3 peptide had largest average RMSD score with native M^{pro} and docked complex was not stable significantly throughout the MD simulation run (Figure 6A). The RMSF plot for the M^{pro} docked and native Cα and side-chain showed an average of 0.88 Å, 1.39 Å, 0.94 Å and 1.44 Å respectively, which denotes the lower atomic fluctuations in binding residues indicating smaller conformational changes (Figure 6B). The total energy, potential energy, RMSD and RMSF analysis revealed that the 2019-nCoV M^{pro} – Remdesivir docking

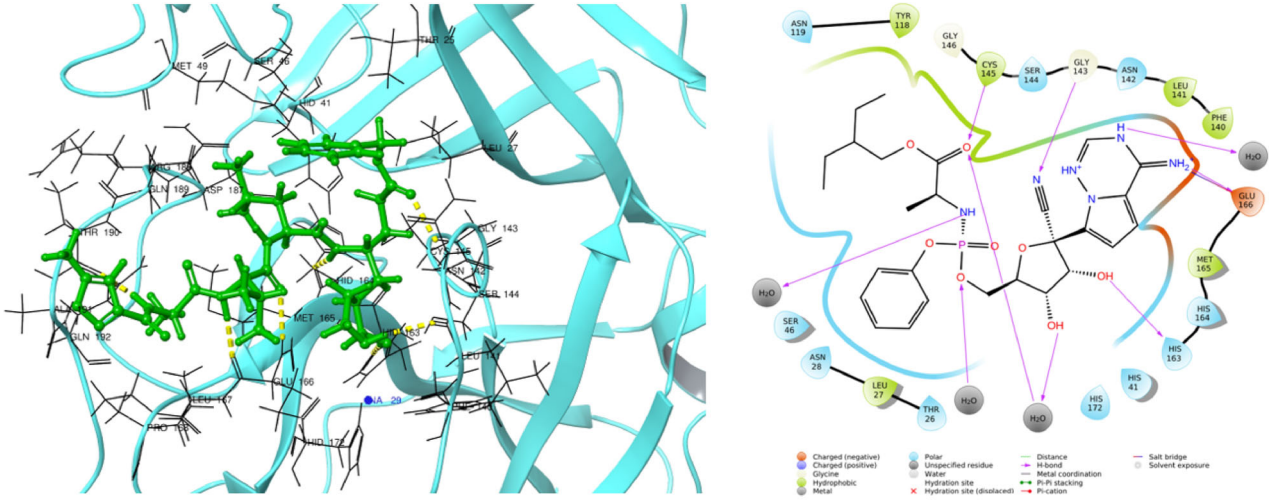

Figure 7. Post MD simulations interactions of docked (M^{pro} – Remdesivir) and native (M^{pro}– N3 peptide) complexes of 2019-nCoV M^{pro} during 100 ns period (A) M^{pro} (cyan) – N3 peptide (green) (B) Molecular interactions of Remdesivir – M^{pro} within 4 Å.

Table 2. H-bond interactions of pre and post molecular dynamics simulations of M^{pro} –Remdesivir and M^{pro} – N3 peptide complex.

	Pre MD simulations		Post MD simulations	
Compound	H-bond	H-bond length (Å)	H-bond	H-bond length (Å)
N3 peptide	Phe140C = O → CN	3.19	–	–
	–	–	Leu141:C = O → NH	2.30
	Gly143:CN → CO	2.87	Gly143:CN → CH	2.42
	Cys145:CS → C = O	2.32	–	–
	His163:CN → C = O	2.37	His163:CN → OH	2.12
	His164:C = O → CN	2.80	His164:C = O → NH	2.26
	Glu166:C = O← CN	2.83	Glu166:C = O← NH	2.00
	Glu166:CN← C = O	2.98	Glu166:C = O← NH	2.40
	Gln189:C = O → CN	2.98	–	–
	Thr190:C = O→ CN	2.85	Thr190:C = O→ CN	1.99
Remdesivir	Pro39:C = O → NH	1.10	–	–
	–	–	Gly143:C≡N → NH	1.86
	Cys145:C = O → NH	2.11	Cys145:C = O ← SH	1.90
	His163:C = O → OH	2.54	His163: OH → C = O	2.84
	His163:NH → C = O	2.13	–	–
	His164:π-π	–	–	–
	Met165:NH → C = O	3.50	–	–
			Glu166:NH → CO	1.56
			Glu166:NH → CO (salt bridge)	1.56
			Five water (HOH) mediated interactions	

complex was highly stable during the entire 100 ns MD simulations.

Remdesivir formed two intermolecular H-bonds with post dynamics structure of M^{pro} residues Gly143, Cys-145 were observed to remain stable in all the trajectories during MD simulations run (Figure 7B and Table 2). Additionally, Glu 166 was formed H-bond and Salt Bridge with M^{pro} and maintained all trajectories. Moreover, four HOH molecules were formed six water-mediated H-bonds with Remdesivir compound (Table 2). The post MD simulations the N3 peptide formed six H-bonds with the native structure residues (5) of Gly143, His163, His164, Glu166, and Thr190 and additionally, Leu141 was formed H-bond with M^{pro} of 2019-nCoV remained stable throughout the period of 100 ns molecular dynamics simulations.

Moreover, similar trends were observed when calculating the rGyr of docked and native complexes (Figure 7A). The rGyr represents the average distance between each atom complexes and the center of mass of the structures and was a useful value to provide a structural measure of the degree of compaction of the studied complexes with MD simulations. Figure 6C depicts the evolution of the rGyr of each complex over the full MD simulations trajectories. The comparison of rGyr average trends towards native and docked depicts 23.66 Å and 22.77 Å, respectively displayed stable over time, suggesting that both complexes have reached a more compact structure (Figure 6C). Whereas, Figure 6D and 6E shows the average SASA of both docked and native has 152.29 $Å^2$ and 161.99 $Å^2$ respectively were observed in 100 ns simulations.

Many ongoing clinical studies also suggests that Remdesivir is much better at inhibiting the SARS-CoV and MERS-CoV. Remdesivir has shown wide therapeutic index and demonstrated anti-viral activity against RNA viruses and

also are selective for viral polymerases along with low susceptibility to cause any human toxicity (Agostini et al., 2018; Sheahan et al., 2020). Drug's delayed chain-termination act is conceived as one of the most crucial mechanisms of action especially in treatment against MERS-CoV and EBOV (Siegel et al., 2017; Jordan et al., 2018; Tchesnokov et al., 2019). In coronaviruses, Remdesivir also exhibited high genetic hurdle resistance and also permits one-time daily dosage because of its extended intracellular half-life (Agostini et al., 2018; Sheahan et al., 2020). This *in silico* study also suggests that Remdesivir has a good docking score with strong binding affinity and stable confirmations with the crucial residues Cys145, and His164 of M^{pro}, which inhibits the replication and proliferation of 2019-nCoV. According to WHO, the recommended administration of Remdesivir for Ebola virus (EBOV) in single or multiple-dose phase intravenous between 3 mg and 225 mg. The risk for central nervous system, respiratory, or cardiovascular effects was considered low at projected therapeutic exposures and is well tolerated without any evidence of kidney or liver toxicity. Moreover, the consistent antiviral activity of Remdesivir for filoviruses (Ebola Zaire, Sudan, Bundibugyo, and Marburg) was observed. Similar antiviral activity was observed also against pathogenic coronaviruses (MERS and SARS CoV) and paramyxoviruses (Nipah and Hendra) discerning for viral polymerases. Thus, the present *in silico* and ongoing clinical studies are also suggesting that the Remdesivir is a potent inhibitor against 2019-nCoV.

Conclusion

The novel human respiratory coronavirus initially called as 2019 – Novel Coronavirus (2019-nCOV) and now called Severe Acute Respiratory Syndrome Coronavirus 2 (SARS-CoV-2) has emphasized the insurgency for therapeutic alternatives to alleviate and stop a novel evolving epidemic of infectious zoonotic diseases. Till now no therapeutic vaccine and drugs against 2019-nCoV are available. Previous epidemics of high-morbidity human coronaviruses, such as SARS-CoV (2003) and MERS-CoV in 2012, motivated the characterization of compounds that could be potentially active against the currently emerging pandemic 2019-nCoV. The most promising compound, Remdesivir currently in clinical trials for treating the EBOV infections, also inhibited the replication of SARS-CoV and MERS-CoV in tissue cultures, and displayed efficacy in non-human animal models. Besides, a combination of the HIV-1 protease inhibitors is shown to be effective in patients infected with SARS-CoV. This *in silico* study also suggested that anti-viral protease inhibitor Remdesivir has the best docking score and binding activity when compared to selected inhibitors and existing peptides with 2019-nCoV of M^{pro}. These inhibitors were tightly bound to the domains I and II cleft of very crucial key residues of Cys145 and His164 of 2019-nCoV, which could inhibit the replication and proliferation in the host, The *in silico* assessment of a single dose with a combination of multiple protease inhibitors against the 2019-nCoV of M^{pro} is the limitation of this study. This study will pave the path for the identification of potential personalized medicine by novel drug designing for different genomic mutations of 2019-nCoV.

Acknowledgements

The authors are highly thankful to the Indian Council of Medical Research (DHR, MoHFW), New Delhi, Government of India, for providing facilities, and resources. MM and NP are highly thankful to TATA trust for providing facilities at the NIN-TATA Centre of Excellence in Public Health and Nutrition, ICMR-National Institute of Nutrition, Hyderabad, Telangana State.

Author contributions statement

Manne Munikumar, Vankudavath Raju Naik and Ungarala Ramakrishna conceived and developed the methods and carried out the analysis of the sequence analysis, molecular docking and dynamics simulations under the supervision of Boiroju Naveen Kumar and Rajkumar Hemalatha. Medithi Srujana, Giridhar Goudar and Naresh Pittla performed literature review, interpreted results, drafted the initial manuscript, and revised the co-authors inputs and additions. All authors revised and reviewed the manuscript.

Disclosure statement

No potential conflict of interest was reported by the author(s).

References

Agostini, M. L., Andres, E. L., Sims, A. C., Graham, R. L., Sheahan, T. P., Lu, X., Smith, E. C., Case, J. B., Feng, J. Y., Jordan, R., Ray, A. S., Cihlar, T., Siege, l D., Mackman, R. L., Clarke, M. O., Baric, R. S., & Denison, M. R. (2018). Coronavirus susceptibility to the antiviral remdesivir (GS-5734) is mediated by the viral polymerase and the proofreading exoribonuclease. *mBio*, *9*(2), 1–15. https://doi.org/10.1128/mBio.00221-18

Anand, K., Ziebuhr, J., Wadhwani, P., Mesters, J. R., & Hilgenfeld, R. (2003). Coronavirus main proteinase (3CLpro) structure: Basis for design of anti-SARS drugs. *Science (New York, N.Y.)*, *300*(5626), 1763–1767. https://doi.org/10.1126/science.1085658

Azam, S. S., & Abbasi, S. W. (2013). Molecular docking studies for the identification of novel melatoninergic inhibitors for acetylserotonin-O-methyltransferase using different docking routines. *Theoretical Biology & Medical Modelling*, *10*(1), 63. https://doi.org/10.1186/1742-4682-10-63

Boopathi, S., Poma, A. B., & Kolandaivel, P. (2020). Novel 2019 coronavirus structure, mechanism of action, antiviral drug promisesand rule out against it treatment. *Journal of Biomolecular Structure and Dynamics*, 1–4. https://doi.org/10.1080/07391102.2020.1758788

Cai, Q., Yang, M., Liu, D., Chen, J., Shu, D., Xia, J., Liao, X., Gu, Y., Cai, Q., Yang, Y., Shen, C., Li, X., Peng, L., Huang, D., Zhang, J., Zhang, S., Wang, F., Liu, J., Chen, L., … Liu, L. (2020). Experimental treatment with favipiravir for COVID-19: An open-label control study. *Engineering*. [In press]. https://doi.org/10.1016/j.eng.2020.03.007

Chen, J. (2020). Pathogenicity and transmissibility of 2019-nCoV-A quick overview and comparison with other emerging viruses. *Microbes and Infection*, *22*(2), 69–71. https://doi.org/10.1016/j.micinf.2020.01.004

Elfiky, A. A. (2020). Natural products may interfere with SARS-CoV-2 attachment to the host cell. *Journal of Biomolecular Structure and Dynamics*, 1–16. https://doi.org/10.1080/07391102.2020.1761881

Felsenstein, J. (1985). Confidence limits on phylogenies: An approach using the bootstrap. *Evolution; International Journal of Organic Evolution*, *39*(4), 783–791. https://doi.org/10.1111/j.1558-5646.1985.tb00420.x

Harrison, C. (2020). Coronavirus puts drug repurposing on the fast track. *Nature Biotechnology*, *38*(4), 379–381. https://doi.org/10.1038/d41587-020-00003-1

Hasan, A., Paray, B. A., Hussain, A., Qadir, F. A., Attar, F., & Aziz, F. M. (2020). A review on the cleavage priming of the spike protein on coronavirus by angiotensin-converting enzyme-2 and furin. *Journal of Biomolecular Structure and Dynamics*, 1–9.

Hay, A. J., Gregory, V., Douglas, A. R., & Lin, Y. P. (2001). The evolution of human influenza viruses. *Philosophical Transactions of the Royal Society of London. Series B, Biological Sciences*, *356*(1416), 1861–1870. https://doi.org/10.1098/rstb.2001.0999

Higgins, D. G., & Sharp, P. M. (1988). CLUSTAL: A package for performing multiple sequence alignment on a microcomputer. *Gene*, *73*(1), 237–244. https://doi.org/10.1016/0378-1119(88)90330-7 https://doi.org/10.1016/0378-1119(88)90330-7

Hilgenfeld, R. (2014). From SARS to MERS: Crystallographic studies on coronaviral proteases enable antiviral drug design. *The FEBS Journal*, *281*(18), 4085–4096. https://doi.org/10.1111/febs.12936

Holshue, M. L., DeBolt, C., Lindquist, S., Lofy, K. H., Wiesman, J., Bruce, H., Spitters, C., Ericson, K., Wilkerson, S., Tural, A., Diaz, G., Cohn, A., Fox, L., Patel, A., Gerber, S. I., Kim, L., Tong, S., Lu, X., Lindstrom, S., … Pillai, S. K. (2020). First case of 2019 novel coronavirus in the United States. *The New England Journal of Medicine*, *382*(10), 929–936. https://doi.org/10.1056/NEJMoa2001191

Huang, C., Wang, Y., Li, X., Ren, L., Zhao, J., Hu, Y., Zhang, L., Fan, G., Xu, J., Gu, X., Cheng, Z., Yu, T., Xia, J., Wei, Y., Wu, W., Xie, X., Yin, W., Li, H., Liu, M., … Cao, B. (2020). Clinical features of patients infected with 2019 novel coronavirus in Wuhan. *The Lancet*, *395*(10223), 497–506. https://doi.org/10.1016/S0140-6736(20)30183-5

Jin, Z., Du, X., Xu, Y., Deng, Y., Liu, M., Zhao, Y., Zhang, B., Li, X., Zhang, L., Peng, C., Duan, Y., Yu, J., Wang, L., Yang, K., Liu, F., Jiang, R., Yang, X., You, T., Liu, X., … Yang, H. (2020). Structure of Mpro from COVID-19 virus and discovery of its inhibitors. *Nature*, *582*(7811), 289–293. https://doi.org/10.1038/s41586-020-2223-y

Jordan, P. C., Liu, C., Raynaud, P., Lo, M. K., Spiropoulou, C. F., Symons, J. A., Beigelman, L., & Deval, J. (2018). Initiation, extension, and termination of RNA synthesis by a paramyxovirus polymerase. *PLoS Pathogens*, *14*(2), e1006889. https://doi.org/10.1371/journal.ppat.1006889

Khandare, A. L., Validandi, V., Manne, M., Reddy, G. B., Kumar Putcha, U., & Gourineni, S. R. (2018). Tamarind fruit extract ameliorates fluoride toxicity by upregulating carbonic anhydrase II: A mechanistic study. *Fluoride*, *51*(2), 137–152.

Killerby, M. E., Biggs, H. M., Haynes, A., Dahl, R. M., Mustaquim, D., Gerber, S. I., & Watson, J. T. (2018). Human coronavirus circulation in the United States 2014–2017. Journal of Clinical Virology, *101*, 52–56. https://doi.org/10.1016/j.jcv.2018.01.019

Kumar, B., Asha, K., Khanna, M., Ronsard, L., Meseko, C. A., & Sanicas, M. (2018). The emerging influenza virus threat: Status and new prospects for its therapy and control. *Archives of Virology*, *163*(4), 831–844. https://doi.org/10.1007/s00705-018-3708-y

Kumar, S., Stecher, G., Li, M., Knyaz, C., & Tamura, K. (2018). MEGA X: Molecular evolutionary genetics analysis across computing platforms. *Molecular Biology and Evolution*, *35*(6), 1547–1549. https://doi.org/10.1093/molbev/msy096

Lee, T. W., Cherney, M. M., Huitema, C., Liu, J., James, K. E., Powers, J. C., Eltis, L. D., & James, M. N. G. (2005). Crystal structures of the main peptidase from the SARS coronavirus inhibited by a substrate-like aza-peptide epoxide. *Journal of Molecular Biology*, *353*(5), 1137–1151. https://doi.org/10.1016/j.jmb.2005.09.004

Leimkuhler, B. J., & Sweet, C. R. (2004). The canonical ensemble via symplectic integrators using Nosé and Nosé-Poincaré chains. *The Journal of Chemical Physics*, *121*(1), 108–116. https://doi.org/10.1063/1.1740753

Lu, H. (2020). Drug treatment options for the 2019-new coronavirus (2019-nCoV). *Bioscience Trends*, *14*(1), 69–71. https://doi.org/10.5582/bst.2020.01020

Luytjes, W., Bredenbeek, P. J., Noten, A. F. H., Horzinek, M. C., & Spaan, W. J. M. (1988). Sequence of mouse hepatitis virus A59 mRNA 2: Indications for RNA recombination between coronaviruses and influenza C virus. *Virology*, *166*(2), 415–422. https://doi.org/10.1016/0042-6822(88)90512-0 https://doi.org/10.1016/0042-6822(88)90512-0

Lu, R., Zhao, X., Li, J., Niu, P., Yang, B., Wu, H., Wang, W., Song, H., Huang, B., Zhu, N., Bi, Y., Ma, X., Zhan, F., Wang, L., Hu, T., Zhou, H., Hu, Z., Zhou, W., Zhao, L., … Tan, W. (2020). Genomic characterisation and epidemiology of 2019 novel coronavirus: Implications for virus origins and receptor binding. *The Lancet*, *395*(10224), 565–574. https://doi.org/10.1016/S0140-6736(20)30251-8 https://doi.org/10.1016/S0140-6736(20)30251-8

Medhi, B., Prajapat, M., Sarma, P., Shekhar, N., Avti, P., Sinha, S., Kaur, H., Kumar, S., Bhattacharyya, A., Kumar, H., & Bansal, S. (2020). Drug targets for corona virus: A systematic review. *Indian Journal of Pharmacology*, *52*(1), 56–65. https://doi.org/10.4103/ijp.IJP_115_20

Morris, G. M., Ruth, H., Lindstrom, W., Sanner, M. F., Belew, R. K., Goodsell, D. S., & Olson, A. J. (2009). Software news and updates AutoDock4 and AutoDockTools4: Automated docking with selective receptor flexibility. *Journal of Computational Chemistry*, *30*(16), 2785–2791. https://doi.org/10.1002/jcc.21256

Munikumar, M., Natarajan, P., Amineni, U., & Radha Krishna, K. V. (2019). Discovery of potential lumazine synthase antagonists for pathogens involved in bacterial meningitis: In silico study. *Informatics in Medicine Unlocked*, *15*, 100187. https://doi.org/10.1016/j.imu.2019.100187

Pant, S., Singh, M., Ravichandiran, V., Murty, U. S. N., & Srivastava, H. K. (2020). Peptide-like and small-molecule inhibitors against Covid-19. *Journal of Biomolecular Structure and Dynamics*, 1–15. https://doi.org/10.1080/07391102.2020.1757510

Pradhan, D., Priyadarshini, V., Munikumar, M., Swargam, S., Umamaheswari, A., & Bitla, A. (2014). Para-(benzoyl)-phenylalanine as a potential inhibitor against LpxC of Leptospira spp.: Homology modeling, docking, and molecular dynamics study. *Journal of Biomolecular Structure & Dynamics*, *32*(2), 171–185. https://doi.org/10.1080/07391102.2012.758056

Rathi, S., Ish, P., Kalantri, A., & Kalantri, S. (2020). Hydroxychloroquine prophylaxis for COVID-19 contacts in India. *Lancet Infectious Diseases*. [In press]. https://doi.org/10.1016/S1473-3099(20)30313-3

Sheahan, T. P., Sims, A. C., Leist, S. R., Schäfer, A., Won, J., Brown, A. J., Montgomery, S. A., Hogg, A., Babusis, D., Clarke, M. O., Spahn, J. E., Bauer, L., Sellers, S., Porter, D., Feng, J. Y., Cihlar, T., Jordan, R., Denison, M. R., & Baric, R. S. (2020). Comparative therapeutic efficacy of remdesivir and combination lopinavir, ritonavir, and interferon beta against MERS-CoV. *Nature Communications*, *11*(1), 222. https://doi.org/10.1038/s41467-019-13940-6

Siegel, D., Hui, H. C., Doerffler, E., Clarke, M. O., Chun, K., Zhang, L., Neville, S., Carra, E., Lew, W., Ross, B., Wang, Q., Wolfe, L., Jordan, R., Soloveva, V., Knox, J., Perry, J., Perron, M., Stray, K. M., Barauskas, O., … Mackman, R. L. (2017). Discovery and synthesis of a phosphoramidate prodrug of a pyrrolo[2,1-f][triazin-4-amino] adenine C-nucleoside (GS-5734) for the treatment of Ebola and emerging viruses. Journal of Medicinal Chemistry, *60*(5), 1648–1661. https://doi.org/10.1021/acs.jmedchem.6b01594

Sliwoski, G., Kothiwale, S., Meiler, J., & Lowe, E. W. (2014). Computational methods in drug discovery. *Pharmacological Reviews*, *66*(1), 334–395. https://doi.org/10.1124/pr.112.007336

Tchesnokov, E. P., Feng, J. Y., Porter, D. P., & Gotte, M. (2019). Mechanism of inhibition of Ebola virus RNA-dependent RNA polymerase by remdesivir. *Viruses*, *11*(4), 326. https://doi.org/10.3390/v11040326

Ton, A.-T., Gentile, F., Hsing, M., Ban, F., & Cherkasov, A. (2020). Rapid identification of potential inhibitors of SARS-CoV-2 main protease by deep docking of 1.3 billion compounds. *Molecular Informatics*, *39*, 2000028. https://doi.org/10.1002/minf.202000028

Umamaheswari, A., Kumar, M. M., Pradhan, D., & Marisetty, H. (2011). Docking studies towards exploring antiviral compounds against envelope protein of yellow fever virus. *Interdisciplinary Sciences, Computational Life Sciences*, *3*(1), 64–77. https://doi.org/10.1007/s12539-011-0064-y

Vilar, S., Karpiak, J., Berk, B., & Costanzi, S. (2011). In silico analysis of the binding of agonists and blockers to the β2-adrenergic receptor. *Journal of Molecular Graphics & Modelling*, *29*(6), 809–817. https://doi.org/10.1016/j.jmgm.2011.01.005

Vincent, M. J., Bergeron, E., Benjannet, S., Erickson, B. R., Rollin, P. E., Ksiazek, T. G., Seidah, N. G., & Nichol, S. T. (2005). Chloroquine is a

potent inhibitor of SARS coronavirus infection and spread. *Virology Journal*, *2*(1), 69. https://doi.org/10.1186/1743-422X-2-69

Wang, M., Cao, R., Zhang, L., Yang, X., Liu, J., Xu, M., Shi, Z., Hu, Z., Zhong, W., & Xiao, G. (2020). Remdesivir and chloroquine effectively inhibit the recently emerged novel coronavirus (2019-nCoV) in vitro. *Cell Research*, *30*(3), 269–271. https://doi.org/10.1038/s41422-020-0282-0

Yang, Y., Peng, F., Wang, R., Guan, K., Jiang, T., Xu, G., Sun, J., & Chang, C. (2020). The deadly coronaviruses: The 2003 SARS pandemic and the 2020 novel coronavirus epidemic in China. *Journal of Autoimmunity*, *109*, 102434. https://doi.org/10.1016/j.jaut.2020.102434

Yu, F., Du, L., Ojcius, D. M., Pan, C., & Jiang, S. (2020). Measures for diagnosing and treating infections by a novel coronavirus responsible for a pneumonia outbreak originating in Wuhan, China. *Microbes and Infection*, *22*(2), 74–79. https://doi.org/10.1016/j.micinf.2020.01.003

Zhang, L., Lin, D., Sun, X., Curth, U., Drosten, C., Sauerhering, L., Becker, S., Rox, K., & Hilgenfeld, R. (2020). Crystal structure of SARS-CoV-2 main protease provides a basis for design of improved α-ketoamide inhibitors. *Science (New York, N.Y.).)*, *368*(6489), 409–412. https://doi.org/10.1126/science.abb3405

Zhu, N., Zhang, D., Wang, W., Li, X., Yang, B., Song, J., Zhao, X., Huang, B., Shi, W., Lu, R., Niu, P., Zhan, F., Ma, X., Wang, D., Xu, W., Wu, G., Gao, G. F., & Tan, W. (2020). A novel coronavirus from patients with pneumonia in China, 2019. *New England Journal of Medicine*, *382*(8), 727–733. https://doi.org/10.1056/NEJMoa2001017